Eur. Phys. J. B **57**, 291–297 (2007)
DOI: 10.1140/epjb/e2007-00163-x

THE EUROPEAN PHYSICAL JOURNAL B

DFT study of $BaTiO_3$ (001) surface with O and O_2 adsorption

G. Rakotovelo[1,2], P.S. Moussounda[1,3], M.F. Haroun[1], P. Légaré[1], A. Rakotomahevitra[2], and J.C. Parlebas[4,a]

[1] Laboratoire des Matériaux, Surfaces et Procédés pour la Catalyse (LMSPC[b]), UMR 7515, CNRS-ECPM, Université Louis Pasteur, 25 rue Becquerel, 67087 Strasbourg Cedex 2, France
[2] Département de Physique, Faculté des Sciences, Université de Mahajanga, BP 652, 401 Mahajanga, Madagascar
[3] Groupe de Simulations Numériques en Magnétisme et Catalyse, Département de Physique, Faculté des Sciences, Université Marien Ngouabi, BP 69, Brazzaville, Congo
[4] Institut de Physique et Chimie des Matériaux de Strasbourg (IPCMS), UMR 7504, CNRS, Université Louis Pasteur, 23 rue du Loess, BP 43, 67034 Strasbourg Cedex 2, France

Received 15 December 2006 / Received in final form 20 March 2007
Published online 6 June 2007 –

Abstract. Progress of scanning tunneling microscopy (STM) allowed to handle various molecules adsorbed on a given surface. New concepts emerged with molecules on surfaces considered as nano machines by themselves. In this context, a thorough knowledge of surfaces and adsorbed molecules at an atomic scale is thus particularly invaluable. In this work, within the framework of density functional theory (DFT), we present an electronic and structural ab initio study of a $BaTiO_3$ (001) surface (perovskite structure) in its paraelectric phase. As far as we know the atomic and molecular adsorption of oxygen at surface is then analyzed for the first time in the literature. Relaxation is taken into account for several layers. Its analysis for a depth of at least four layers enables us to conclude that a reasonable approximation for a $BaTiO_3$ (001) surface is provided with a slab made up of nine plans. The relative stability of two possible terminations is considered. By using a kinetic energy cut off of 400 eV, we found that a surface with BaO termination is more stable than with TiO_2 termination. Consequently, a surface with BaO termination was chosen to adsorb either O atom or O_2 molecule and the corresponding calculations were performed with a coverage 1 on a (1×1) cell. A series of cases with O_2 molecule adsorbed in various geometrical configurations are also analyzed. For O_2, the most favorable adsorption is obtained when the molecule is placed horizontally, with its axis, directed along the Ba-Ba axis and with its centre of gravity located above a Ba atom. The corresponding value of the adsorption energy is -9.70 eV per molecule (-4.85 eV per O atom). The molecule is then rather extended since the O–O distance measures 1.829 Å. By comparison, the adsorption energy of an O atom directly located above a Ba atom is only -3.50 eV. Therefore we are allowed to conclude that the O–O interaction stabilizes atomic adsorption. Also the local densities of states (LDOS) corresponding to various situations are discussed in the present paper. Up to now, we are not aware of experimental data to be compared to our calculated results.

PACS. 73.20.Hb Impurity and defect levels; energy states of adsorbed species – 71.15.Mb Density functional theory, local density approximation, gradient and other corrections

1 Introduction

Since last decades, technology has been completely changed because of data processing. Also, thanks to the power of large computers, exploration of nano structures world has been push further significantly. Oxides with perovskite structures exhibit various interesting properties. Barium titanate compounds, for example, are ferroelectric wide band gap semiconductors. They are used in many applications, such as non-volatile ferroelectric memory and varistors, in protection circuits in order to prevent thermal overload. Large capacity memory devices put this type of phenomenon into the group of hot topics in modern solid state physics. The development of up to date theoretical surface science provides an opportunity to investigate surfaces and adsorbate structures at the atomic scale with useful applications in industrial technologies. It is also especially convenient to improve our understanding of surface chemistry process as catalysis.

Many studies were already performed concerning atomic and electronic structures of $BaTiO_3$ surfaces. See

[a] e-mail: parlebas@ipcms.u-strasbg.fr
[b] LMSPC is a partner of the European Laboratory for Catalysis and Surface Science (ELCASS).

for example Heifets et al. [1] for a study of $BaTiO_3$ surface polarization. Padilla et al. [2] explored the ferroelectricity, the structure and the energy of $BaTiO_3$ tetragonal and cubic phases. Iniguez et al. [3] treated the $BaTiO_3$ temperature-pressure phase diagram. Also Xue et al. [4] investigated the surface energy in the paraelectric state. All these studies were concerned by the physical properties of the considered mixed oxides. However, their surface chemical properties are still almost unknown, although this is an important issue determining their general behavior and stability. Especially, there is a lack of information concerning their surface state in contact with atmosphere. $BaTiO_3$ type systems can also be considered as catalysts or catalyst supports and a detailed knowledge of their interaction with various molecules is then needed. In this respect, we note a recent experimental study of CO and CO_2 interactions with $SrTiO_3$ (001) [5], but no related theoretical work has been published yet.

Here we present a study of physico-chemical properties of a (100) surface of $BaTiO_3$ using density functional theory (DFT). As we are mainly concerned by surface reactions which could be part of a catalytic mechanism, we focus on the cubic phase of $BaTiO_3$ which is a stable phase above room temperature [3]. We first examine the relative stabilities of two possible surface terminations. We then consider the interaction of the most stable surface with atomic and molecular oxygen. Our paper is organized as follows. In Section 2, details of our data processing method are described. The results of our DFT calculations for the surface energy as well as O and O_2 adsorption on a $BaTiO_3$ (001) face are given in Section 3 along with the interpretation of the corresponding local densities of states (LDOS). Discussion and conclusion are developed in the last Section 4.

2 Computational methods

The quantum chemical calculations reported in this paper were performed using a Dacapo package [6] for periodical systems. This program is based on DFT. It uses a plane wave basis set. Ionic cores are described by ultrasoft pseudo potentials [7]. The Kohn-Sham one electron equations are solved self-consistently. In our calculations, the Perdew-Wang functional (PW91) was used in the generalized gradient approximation (GGA) [8]. Also a Monkhorst-Pack scheme generated all the k-points. Calculations on a $BaTiO_3$ (001) (1×1) slab were performed with a $6 \times 6 \times 1$ mesh in k-space. A 400 eV high energy cut off was introduced for the plane wave set in all calculations. A Fermi broadening corresponding to $k_BT = 0.1$ eV was used to help convergence. All total energies have been extrapolated to $T = 0$ K. The results presented in this paper were obtained with spin unpolarised calculations. However, spin polarized calculations were conducted on both the clean surface and the molecularly adsorbed O_2. No difference with unpolarized calculations was revealed. Only the reference calculation concerned with a free O_2 molecule needed the help of spin polarization. The electronic structure was studied by using LDOS curves obtained by projection on an atomic basis. The partial and total electron count on individual atoms is thus deduced by integration. In order to avoid double electron counting due to short Ba–O bonds during O and O_2 adsorption, the projection was performed in a sphere limited by a 0.7 Å radius.

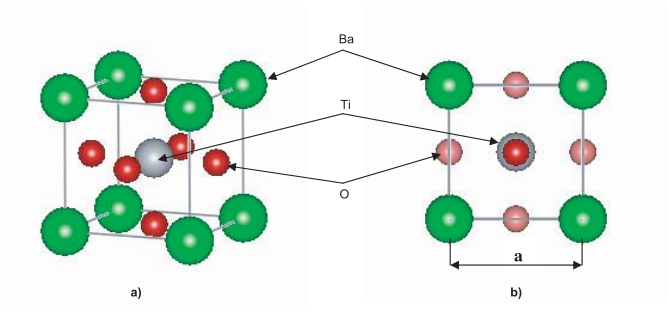

Fig. 1. Cubic phase of $BaTiO_3$, (a) 3D sight showing the superposition of the two alternate BaO and TiO_2 layers; (b) top view of a $BaTiO_3$ (001) surface.

Before starting the surface calculation, we tested DFT method by calculating the lattice constant a of bulk cubic $BaTiO_3$ perovskite crystal (Fig. 1). We obtained $a = 3.978$ Å, which is rather close to the experimental reference (3.996 Å) as well as theoretical calculations [4] (see Tab. 1). Let us just point out that in reference [2] the computed lattice constant is somewhat smaller than the experimental one and this underestimation is typical of a LDA calculation. In the [001] direction, $BaTiO_3$ can be seen as an alternate packing of planes corresponding respectively to BaO and TiO_2 formulas (see Fig. 1). Consequently, a slab corresponding to $BaTiO_3$ formula exhibits one BaO surface and one TiO_2 surface. Therefore the energy involved in the creation of a (001) surface by cleaving $BaTiO_3$ corresponds to the simultaneous creation of these two surfaces. In order to determine separately the stability of these two surfaces, we had to use $(BaO)_n(TiO_2)_m$ slabs where $\Delta n = n - m = \pm 1$. When $\Delta n = +1(-1)$ the slab exhibits two BaO (TiO_2) terminations. In the calculations, the total number of planes $(n+m)$ was equal to 9 as represented in Figure 2. The images of the slabs were separated by a vacuum space equivalent to a ten interlayer space. In order to keep slab symmetry for surface energy calculations, the central plane was settled in a fixed position whereas the 4 planes on the two sides were allowed to relax symmetrically. In order to check the convergence of our calculations with respect to slab thicknesses, a clean surface study was also performed with a 11 layers slab. In that case, the 3 central layers were frozen. For the adsorption studies presented here, we used a (1×1) surface unit mesh with 9 planes BaO-terminated slab. The adsorbates were adsorbed on one face only, and the 4 planes below were allowed to relax. The 5 other planes were frozen. In order to compensate the asymmetry of the system, a dipole was introduced in the vacuum region, hence decoupling the various slab images [10].

A series of models were treated involving O atom and O_2 molecule adsorbed in various configurations. In all the

Table 1. Comparison of our calculated value of the cell parameter "a" to experimental and theoretical values.

Parameter (Å)	Expt Reference [8]	Theoretical value		
		Reference [2]	Reference [4]	Our value
a	3.996	3.948	3.977	3.978

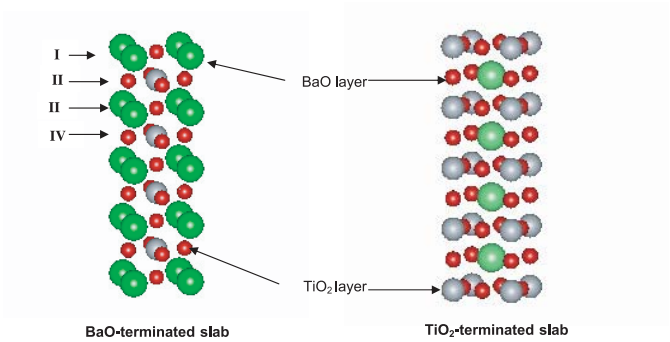

Fig. 2. Representation of 9-layers slab of $BaTiO_3$ (001) with BaO termination (left) and TiO_2 termination (right). The 4 layers which are freely relaxed are indicated with arrows.

results given here, the adsorption energy is defined with respect to a free O_2 molecule and a clean relaxed slab. Negative adsorption energy corresponds to a stable adsorbate-substrate system.

3 Results and discussions

3.1 Relaxation effect

We present in Tables 2 and 3 the result of symmetric and asymmetric relaxations for 9 and 11 layers thick slabs with BaO and TiO_2 terminations respectively. Whereas the former type of relaxation was necessary for our stability comparison of BaO and TiO_2-terminated surfaces, the latter was preferred for adsorbate studies. The various calculations agree on both sign and amplitude of the interlayer space variations. From Tables 2 and 3 and for d_{12}, d_{23} and d_{34} respectively, we obtain the following results with their dispersions: -0.140 ± 0.001 Å, 0.080 ± 0.002 Å and -0.033 ± 0.001 Å in the case of BaO-terminated slabs and -0.149 ± 0.004 Å, 0.091 ± 0.001 Å and -0.036 ± 0.005 Å in the case of TiO_2-terminated slabs . Our d_{12} contraction is somewhat larger but in agreement with the one reported by Padilla [2] using a thinner slab (7 layers) and a shorter basis cutoff.

Tables 4 and 5 report the rumpling for the 4 first layers of BaO and TiO_2-terminated slabs respectively. Again, a general agreement between the various approaches and with previous studies [2] is found. Negative and positive rumpling with respect to O atoms alternate from the surface layer for both terminations. We note that the amplitude of rumpling is about –5% for a BaO surface layer and strongly damped in layers below. On the contrary, on the TiO_2-terminated slab, the strongest buckling appears in the first BaO layer below the TiO_2 surface.

As a conclusion, we used symmetrically relaxed 11 layers slabs for our surface stability study. However the surface behavior is nicely reproduced by asymmetrically relaxed 9 layers slabs which were used for adsorption studies.

3.2 Surface energy

We used Padilla's method [2] to obtain the surface energy and compare the stabilities of both terminations. We calculated the formation energy of bulk $BaTiO_3$ by starting from the bulk forms of TiO_2 (rutile) and BaO according to the reaction:

$$\mathrm{BaO} + \mathrm{TiO_2} \longrightarrow \mathrm{BaTiO_3}.$$

The formation energy is defined as:

$$E_f = E_{\mathrm{BaTiO_3}} - [E_{\mathrm{BaO}} + E_{\mathrm{TiO_2}}].$$

The three right-hand terms were calculated in similar conditions (same cutoff, pseudopotentials, and adapted k-point grids) and the unit mesh parameters were optimized for each compound. For TiO_2, the rutile phase was considered. E_f was found to be -1.51 eV. We note that the formation energy reported in [2] for the tetragonal phase is clearly lower (-3.23 eV) as can be expected for the most stable phase at low temperature. By defining the variation of the free Gibbs enthalpy, ΔG, according to the formation energy and the chemical potentials, μ_{BaO} and $\mu_{\mathrm{TiO_2}}$, we get the following equation:

$$\Delta G = E_f - [\mu_{\mathrm{BaO}} + \mu_{\mathrm{TiO_2}}]$$

$\mu_{\mathrm{BaTiO_3}} = 0$ corresponds to the origin of chemical potentials. If $BaTiO_3$ is in balance with BaO and TiO_2, we have:

$$E_f = \mu_{\mathrm{BaO}} + \mu_{\mathrm{TiO_2}}.$$

The surface Gibbs free enthalpy per surface unit cell is then [2]

$$\Delta G_{surface} = 1/2[E_{slab} - n(E_{\mathrm{BaO}} + \mu_{\mathrm{BaO}}) - m(E_{\mathrm{TiO_2}} + \mu_{\mathrm{TiO_2}})]$$

which stands for the BaO (TiO2)-terminated slab when $\Delta n = +1\,(-1)$ and E_{slab} is the DFT total energy of the corresponding slab. By varying $\mu_{\mathrm{TiO_2}}$ between the values of E_f and 0, we obtain the energy of a $BaTiO_3$ (001) surface (Fig. 3). We observe that the BaO-terminated surface is the most stable in the whole composition range although the TiO_2-terminated surface approaches similar energy in the TiO_2 rich region. The mean values of the BaO (TiO_2) -terminated surface is 0.480 (1.365) eV/surface cell. Again this is in contrast with the results reported in [2] where the two terminations of both tetragonal and cubic phases

Table 2. Surface relaxation of 9 layers and 11 layers BaO-terminated slabs. For symmetric relaxation 4 layers were free to relax on each face of the slab. In asymmetric relaxation, 4 layers were free to relax, the rest being frozen at bulk position. Δd_{ij} is the distance change between two consecutive layers mean position; percentage is calculated with respect to the bulk interlayer space: $\Delta d_{ij} = [z(\mathrm{M})_i + z(\mathrm{O})_i]/2 - [z(\mathrm{M})_j + z(\mathrm{O})_j]/2$.

Layers	Symmetric relaxation				Asymmetric relaxation			
	9 layers		11 layers		9 layers		11 layers	
	Δd_{ij} (Å)	%	Δd_{ij} (Å)	%	Δd_{ij} (Å)	%	Δd_{ij} (Å)	%
I–II	−0.139	−6.97	−0.139	−6.79	−0.140	−7.04	−0.132	−6.62
II–III	0.081	4.09	0.078	3.77	0.078	2.92	0.063	3.20
III–IV	−0.031	−1.55	−0.031	−1.11	−0.035	−1.76	−0.032	−1.62

Table 3. Surface relaxation of 9 layers and 11 layers TiO_2-terminated slabs. For symmetric relaxation 4 layers were free to relax on each face of the slab. In asymmetric relaxation, 4 were free to relax, the rest being frozen at bulk position. Δd_{ij} is the distance change between two consecutive layers mean position; percentage is calculated with respect to the bulk interlayer space: $\Delta d_{ij} = [z(\mathrm{M})_i + z(\mathrm{O})_i]/2 - [z(\mathrm{M})_j + z(\mathrm{O})_j]/2$.

Layers	Symmetric relaxation				Asymmetric relaxation			
	9 layers		11 layers		9 layers		11 layers	
	Δd_{ij} (Å)	%	Δd_{ij} (Å)	%	Δd_{ij} (Å)	%	Δd_{ij} (Å)	%
I–II	−0.145	−7.30	−0.146	−7.34	−0.153	−7.70	−0.143	−7.12
II–III	0.090	4.52	0.080	4.02	0.092	4.64	0.071	3.56
III–IV	−0.031	−1.56	−0.036	−1.81	−0.042	−2.10	−0.021	−1.04

Table 4. Surface rumpling ΔZ of the BaO-terminated slab defined by $\Delta z = [z(\mathrm{M}) - z(\mathrm{O})]$. Percentage is calculated with respect to the bulk interlayer space.

Layers	Symmetric relaxation				Asymmetric relaxation			
	9 layers		11 layers		9 layers		11 layers	
	ΔZ (Å)	%	ΔZ (Å)	%	ΔZ (Å)	%	ΔZ (Å)	%
I (BaO)	−0.110	−5.51	−0.110	−5.51	−0.112	−5.62	−0.101	−5.08
II (TiO_2)	0.022	1.10	0.022	1.09	0.023	1.14	0.015	0.75
III (BaO)	−0.035	−1.77	−0.033	−1.67	−0.040	−2.01	−0.028	−1.40
IV (TiO_2)	0.006	0.29	0.005	0.26	0.009	0.43	0.00	0.01

are roughly similarly stable, the mean values amounting to 1.237 eV and 1.241 eV respectively. The discrepancy was already obvious in the evaluation of the $BaTiO_3$ formation energy. Clearly, this points to differences in the computation of the bulk energies of $BaTiO_3$, TiO_2 and BaO. LDA as used in [2] tends to underestimate the equilibrium mesh parameters. In this point of view, GGA as used in this work is more correct, as shown in Table 1. Other computational conditions could pledge in favor of a better accuracy in the present work: (i) we used a 400 eV cutoff which is certainly better for oxygen containing materials than the 340 eV cutoff used in [2]; (ii) our k-point mesh was (6×6×1) against (4×4×2) in [2]. This altogether could account for differences in the tenth of eV range for the energy of each compound. The uncertainties cumulates in $BaTiO_3$ formation energy resulting of the sum of three terms. Yet a 100% difference between the two computations remains puzzling. The situation is even worst for the surface energy where each uncertainty is somehow multiplied by the number of BaO and TiO_2 layers in the slab. This discussion at least shows that the comparative stabilities of the two surface terminations should be taken with care.

Another approach of the surface stabilities was used in the literature [11]. It relies on a starting calculation of

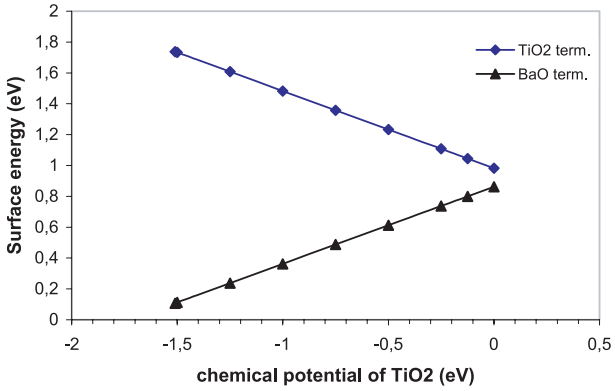

Fig. 3. Surface energy as a function of the chemical potential μ_{TiO_2} for the two types of $BaTiO_3$ (001) surfaces, in the cubic phase and for a 9-layers slab.

half the surface energy of an unrelaxed stoechiometric slab (i.e. with both terminations) reduced by the energy gain obtained by relaxing either the BaO or TiO_2 face. From our calculations, this gives 0.962 (0.884) eV/surface cell for the BaO (TiO_2)-terminated surface respectively. This is in agreement with DFT calculations recently published on the same system [12]. This confirms that the relaxation is more efficient for a TiO_2 than for a BaO face of

Table 5. Surface rumpling ΔZ of the TiO_2-terminated slab defined by $\Delta z = [z(\mathrm{M}) - z(\mathrm{O})]$. Percentage is calculated with respect to the bulk interlayer space.

Layers	Symmetric relaxation				Asymmetric relaxation			
	9 layers		11 layers		9 layers		11 layers	
	ΔZ (Å)	%	ΔZ (Å)	%	ΔZ (Å)	%	ΔZ (Å)	%
I (TiO_2)	−0.093	−4.67	−0.092	−4.63	−0.101	−5.08	−0.093	−4.68
II (BaO)	0.112	5.65	0.109	5.50	0.122	6.13	0.113	5.68
III (TiO_2)	−0.017	−0.85	−0.014	−0.68	−0.020	−1.01	−0.084	−4.22
IV (BaO)	0.018	0.89	0.020	1.02	0.021	1.06	0.025	1.26

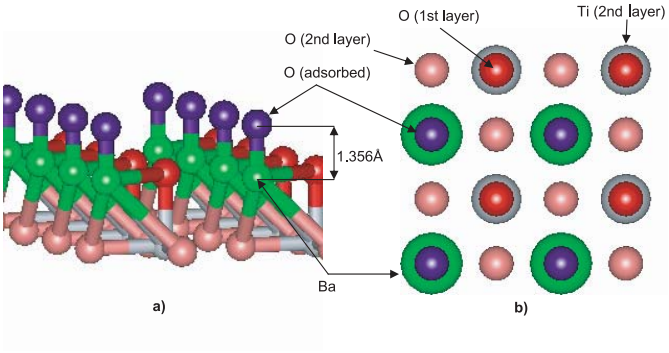

Fig. 4. Adsorption of the oxygen atom on $BaTiO_3$ (001) surface with BaO termination: (a) 3D view; (b) top view with O adsorbed vertically on Ba.

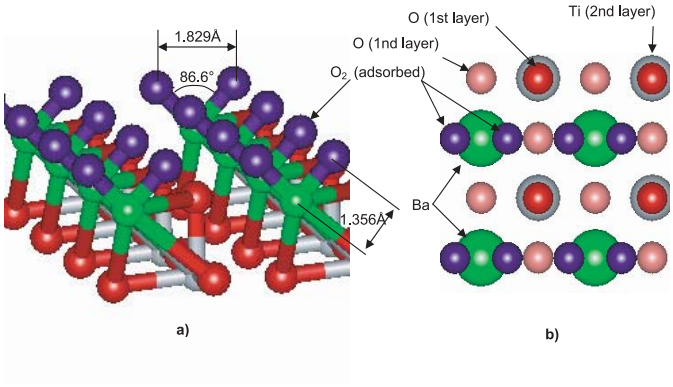

Fig. 5. Adsorption of the O_2 molecule on $BaTiO_3$ (001) surface with BaO termination: (a) 3D view; (b) top view with O_2 adsorbed horizontally above the Ba-Ba axis.

a slab, but does not contradict our above result that a BaO face is fundamentally (thermodynamically) the most stable face before and after surface relaxation. As a consequence of the comparison between two terminations, the adsorption studies presented below were performed on a BaO-terminated slab.

3.3 Adsorption of O and O_2 on a $BaTiO_3$ (001) surface

In our calculations, we tested the O adsorption on top of a Ba atom with a (1×1) surface cell (Fig. 4). We found that there is a strong corresponding adsorption energy of −3.50 eV per O atom with respect to O_2 (Tab. 6). The Ba–O distance is then 1.357 Å. We note that this value is considerably shorter than the in-plane Ba–O distance (2.813 Å) as well as the summation of O^{2-} and Ba^{2+} ionic radius both supposed to be in the range of 1.4 Å.

We then placed an O_2 molecule on top of a Ba atom in the same unit cell. When the molecular axis was oriented vertically, the optimized slab happened to be unstable with respect to a corresponding free molecule. Also we examined the configuration with a O–O axis parallel to the Ba–Ba axis (Ox axis of the model), the center of gravity of the molecule being then exactly on top of Ba. As can be seen in Table 6, the value of the adsorption energy is now −4.85 eV per O atom. The molecule gets very extended with a O–O distance of 1.829 Å and a Ba–O length of 1.336 Å i.e. even shorter than for atomic adsorption. The shortest distance between 2 neighboring molecules is thus 2.149 Å. We note that the comparison of O and O_2 adsorption energies is in line with the chemisorption bond reduction. The OBaO angle is 86.5°. This optimized configuration is represented in Figure 5.

3.4 Density of states analysis

3.4.1 Adsorbed O atom at the top of a Ba site

Figure 6a illustrates the LDOS for adsorbed O atom at the top of a Ba site upon a $BaTiO_3$ (001) surface whereas Figure 6b shows Ba LDOS after adsorption. We note that both curves exhibit resonances around −20, −17, −12, −7, −5 and 1 eV, and a continuous distribution of states from −4 eV to 0 eV This indicates a high covalent character of the formed Ba–O bond. A deeper analysis confirms this conclusion: on both atoms, the −20 eV and −17 eV states are essentially of s character. Actually p_x and p_y character dominates at −12 eV and −5 eV up to 0 eV (with some d_{xz} and d_{yz} contributions for Ba) whereas the −7 eV contribution has essentially a p_z character. Also the unoccupied states around 1 eV presents a p_z character on both atoms, plus a d_{z2} contribution for Ba. In addition, from Figure 6a we notice that the LDOS curve of a chemisorbed O atom clearly differs from the corresponding curve of a surface O atom. This is not surprising since they have very different neighbourhoods. Figure 6b shows that the covered Ba atom is perturbed by the presence of its chemisorbed O atom. States of s character are shifted from −26 eV to −20 eV upon building the new Ba–O bond. The electronic distribution from −5 eV up to 0 eV is also perturbed. Especially, the d character in this

Table 6. Calculated results of the adsorption energy per oxygen atom for O atom and O_2 molecule and comparison of the distance between O atoms in the case of free and adsorbed oxygen molecule.

Adsorbate	d(Ba–O) (Å)	d(O–O) (Å)	$E_{adsorption}$ (eV)
O	1.357		−3.50
O–O (flat position)	1.336	1.829	−4.85
O–O(gas) free		1.236	

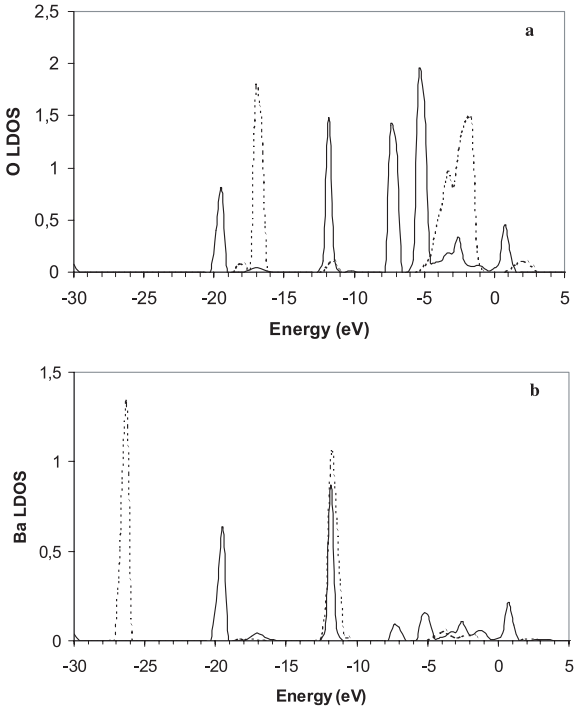

Fig. 6. O atomic adsorption on a BaO-terminated surface. (a) LDOS of an adsorbed O atom on top of Ba (solid curve), and LDOS of an O atom of the clean surface (dashed curve). (b) LDOS of a surface Ba atom after (solid curve) and before (dashed curve) O atomic adsorption. The energy scale is referred to the highest occupied states.

region and around 1 eV is essentially the result of this new bond. We conclude that the O chemisorption bond pulls down the previously unoccupied $4d$ states.

With respect to a clean surface Ba atom, the covered Ba atom loses an important electronic charge (-0.48 e$^-$). This loss of charge is essentially of s character, the rest being of p_z symmetry. In the limited region where we performed the electron count, there is practically no change for the adsorbed oxygen atom, with respect to the electron count in a free O_2 molecule. However, the character of the electrons is modified by adsorption: there is a loss of s states compensated by a gain of p_x and p_y states. When the charge on the adsorbed O atom is compared to one on the free O atom, we find that the adsorbed atom is missing an impressive electron loss of about -0.40 e$^-$. This can be interpreted by considering that the orbitals of a O free atom are contracted with respect to both an O_2 molecule and an adsorbed O atom.

3.5 Adsorbed O_2 molecule at the top of a Ba site

LDOS of an O_2 molecule adsorbed at the top of a Ba site is shown in Figure 7a as well as the corresponding LDOS of a free O_2 molecule. The LDOS curves of a surface Ba atom, after and before O_2 adsorption are presented in Figure 7b. Again, a good correspondence of O and Ba features can be noted in peaks around -26, -20, -17, -14 eV, and some overlapping features from -10 eV up to 0 eV. However, the overall distribution differs clearly from the one in Figure 6. The electronic feature of O_2 chemisorbed molecule corresponds to the one related to a free molecule after a proper shift: the higher the energy, the more important the shift is. This is clearly the consequence of an extended O–O bond, so that the electrons are shared between both bonded O atoms and the Ba atom. Again, an analysis of the character of the various O and Ba features revealed a good correspondence. Especially we point out that the -14 eV peak is essentially of p_y character on both atoms, showing some π interaction. The region from -11 eV to 3 eV is a mixture of $s+p$ states with some d contribution on Ba, specially d_{xz} around 1 eV.

Now we consider the electron transfer induced by the O_2 molecular adsorption. The electron loss (-0.80 e$^-$) for Ba is roughly twice that of the atomic O adsorption. It is principally s states (more than half the net loss), but also p states (mostly p_y, i.e. in the direction perpendicular to the molecular axis, in the surface plane) which are transferred. There is also a limited d gain, essentially in the out of plane (z) direction. There is a net electron gain for oxygen with respect to the free molecule ($+0.31$ e$^-$ per O). However there is a loss of s electrons by half the net gain. In exchange, the gain is of p character, dominated by p_y. We note that the figure is not qualitatively different from that obtained with atomic adsorption.

4 Discussion and conclusion

Our results concerning the structure of a clean (001) surface of $BaTiO_3$ are in good agreement with previously published data [2,4,12] for both BaO and TiO_2 terminations. The respective stabilities of both terminations are compared for the cubic phase. We find that a BaO surface is clearly favored with respect to a TiO_2 termination. This is in contrast to the conclusions drawn (i) from a $BaTiO_3$ tetragonal phase study [2] as well as (ii) on the basis of relaxation efficiency only.

In agreement with the above point, we examined O and O_2 adsorption on the most likely exposed BaO surface. We found that both the atomic or molecular

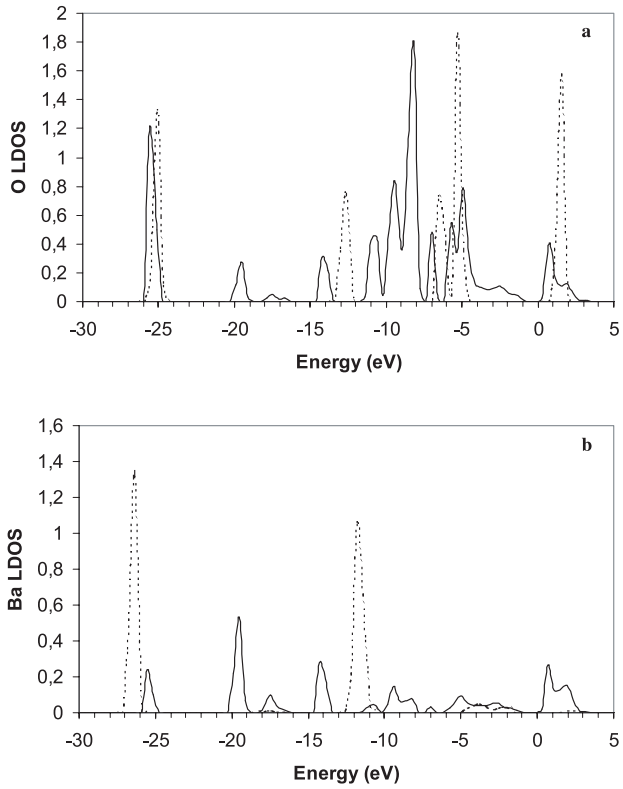

Fig. 7. O_2 adsorption on a BaO-terminated surface. (a) LDOS of an adsorbed O atom (solid curve), and LDOS of an O atom in the free O_2 molecule (dashed curve). (b) LDOS of a surface Ba atom after (solid curve) and before (dashed curve) O_2 adsorption. The energy scale is referred to the highest occupied states.

adsorption energy of oxygen on top of a Ba atom was very high. Surprisingly, O_2 adsorption leads to a bigger adsorption energy (-4.85 eV/O) than the atomic adsorption (-3.50 eV), although the former results in twice the O coverage of the latter. This counterintuitive result can only be understood by considering that there is still a stabilizing interaction between O atoms of an adsorbed O_2 in spite of a considerably extended O–O bond length (1.829 Å). However, it is also necessary that the decrease in O–O stabilization, with respect to the gas phase, is overcompensated by a new mechanism which does not operate for atomic adsorption. This suggests an energy gain due to some electron delocalization running over both O atoms plus the Ba atom. This is in agreement with our analysis of LDOS of O and Ba of O_2 molecular adsorption showing that the main feature of the O_2 electronic structure is conserved together with some clear electron exchange with Ba. This also account for shorter Ba–O bond length for molecular adsorption compared to atomic adsorption.

Finally, we stress that this preliminary study indicates that chemical properties of mixed oxides are of large interests and that a more extended work is still needed.

G. Rakotovelo and P.S. Moussounda address their thanks to the "Service de Coopération et d'Action Culturelle (SCAC) des Ambassades de France à Madagascar et au Congo-Brazzaville", and to the "Agence Universitaire de la Francophonie (AUF)" for their partial financial support. A. Rakotomahevitra is grateful to ICTP (Trieste) for facilitating a stay at IPCMS in order to help G. Rakotovelo at an early stage of his doctorate thesis.

References

1. E. Heifets, S. Dorfman, D. Fuks, E. Kotomin, Thin Solid Films **296**, 76 (1997)
2. J Padilla, D. Vanderbilt, Phys. Rev. B **56**, 1625 (1997)
3. J. Iniguez, D. Vanderbilt, Phys. Rev. Lett. **89**, 115503 (2002)
4. X.Y. Xue, C.L. Wang, W.L. Zhong, Surf. Sci. **550**, 73 (2004)
5. S. Azad, M.H. Engelhard, L.-Q. Wang, J. Phys. Chem. B **109**, 10327 (2005)
6. B Hammer, L.B. Hansen, J.K. Norskov, Phys. Rev. B **59**, 7413 (1999)
7. D. Vanderbilt, Phys. Rev. B **41**, 789 (1990)
8. J.P. Perdew, J.A. Chevary, S.H. Vosko, K.A. Jackson, M.R. Pederson, D.J. Singh, C. Fiolhais, Phys. Rev. B **46**, 6671 (1992)
9. T. Mitsui, S. Nomura, in *Ferroelectrics and Related Substances. Oxides*, edited by K.-H. Hellwege, O. Madelung, Landolt-Börnstein, News Series, Group III, Vol. 16, pt. A (Springer-Verlag, Berlin, 1981)
10. J. Neugebauer, M. Scheffler, Phys. Rev. B **46**, 16067 (1992)
11. E. Heifets, R.I. Eglitis, E.A. Kotomin, J. Maier, G. Borstel, Phys. Rev. B **64**, 235417 (2001)
12. R.I. Eglitis, G. Borstel, E. Heifets, S. Piskunov, J. Electroceram. **16**, 289 (2006)